Neutronic Performance Evaluation of Different Control Rod Materials in Soluble Boron-Free i-SMR Core

Woo Jin Lee ^a , Ser Gi Hong ^{a*}, Jin Sun Kim^{b*}

^a Departments of Nuclear Engineering, Hanyang University, 222, Wangsimni-ro, Seongdong-gu, Seoul, 04761, Republic of Korea

^b KEPCO Nuclear Fuel Co. Ltd., 242, Deadeok-daero 989beon-gil, Yuseong-gu Daejeon, 34507, Republic of Korea

^{a*}Corresponding author: <u>hongsergi@hanyang.ac.k</u>

b*Project manager of the i-SMR technology development project of the Innovative Small Modular Reactor

Development Agency

*Keywords: Soluble-Boron Free i-SMR, Control Rod Material, Core Performance

1. Introduction

Recently, South Korea has been developing i-SMR, which adopts the concept of soluble boron-free (SBF) operation [1]. The SBF operation offers several advantages, such as reduced liquid radioactive waste, simplified chemical and volume control system (CVCS), and enhanced inherent safety due to a more negative moderator temperature coefficient (MTC).

However, operating a SBF core presents significant challenges. Since soluble boron is absent, excess reactivity must be fully managed through control rods (CR) and burnable absorbers (BA). Moreover, the more negative MTC compared to large-scale PWRs, introduces difficulties in maintaining cold zero power (CZP) shutdown margin. The adoption of the TM-ICI (top-mounted in-core instrumentation) concept in i-SMR [1], which limits the number of CRs, further complicates this issue.

During normal operation, withdrawal of CRs near the end of cycle (EOC) may cause severe axial power deviation and localized power increase, leading to risk of pellet-cladding interaction (PCI). In addition, the expanded load-follow requirements for SMRs (e.g., 100-20-100% power ramping) [2] increase CR movement, further adding to these challenges. Therefore, an optimized CR design is important to ensure safe core operation.

CR design parameters include absorber material, overlap strategy, insertion sequence, grouping, and positioning. In this study, a feasibility assessment of candidate CR materials is first conducted under CZP conditions, followed by core performance evaluations under hot full power (HFP) operation.

For the neutronic analysis, the two-step procedure with DeCART2D v1.1 [3] and MASTER v4.0 [4], both developed by KAERI, is employed. DeCART2D generates assembly-wise homogenized group constants using a 47-group neutron and 18-group gamma library (DML-E71N047G018-PV05-APR-CR04-R9.BIN [5]) based on ENDF/B-VII.1, while MASTER performs three-dimensional core nodal diffusion calculations with

the Source Expansion Nodal Method (SENM), supporting both steady-state and transient simulation.

2. Design and Methodologies

2.1 Reactor core design

The SBF i-SMR has a thermal power of 520 MWth, with 69 fuel assemblies (FA) and an active fuel height of 240 cm [1]. The FA utilizes a 17x17 lattice, containing 28 guide tubes for CRs and one instrumentation tube [6]. BAs are implemented using UO₂-Gd₂O₃ enriched with Gd-155 and Gd-157, while the U-235 enrichment of the fuel pellets is 4.0 w/o and 4.95 w/o.

To ensure sufficient shutdown margin, a B₄C shutdown bank enriched with 95% B-10 is employed, whereas excess reactivity is controlled using Ag-In-Cd (AIC) regulation banks. Fig. 1 shows the radial configuration of the regulation banks (R bank) in the i-SMR core. The insertion sequence of regulation banks is $R4 \rightarrow R3 \rightarrow R2 \rightarrow R1$, with an overlap length of 120 cm.

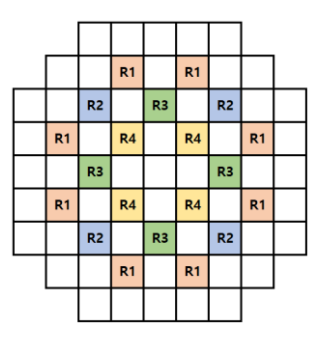


Fig. 1. Radial configuration of regulation CR bank in i-SMR core

2.2 Selection of CR material for sensitivity analysis

The absorption capability and reactivity worth of CRs are highly dependent on their material. As CR worth strongly affects the axial power distribution during CR movements, careful selection of R bank materials is important for the i-SMR core, in which excess reactivity

is managed during both steady-state HFP and load-follow operations.

Accordingly, Table I summarizes the candidate CR materials considered for the sensitivity analysis. The uniform configuration, as illustrated on the left side of Fig. 2, refers to the case where each CR finger is composed of a single absorber material. The candidates include Stainless steel-304 (SS304), Inconel-625, Hafnium (Hf), and AIC which corresponds to the reference design described in Section 2.1, is considered, along with a reduced-radius AIC option within this class.

Table I: Candidate CR materials for sensitivity analysis

Class	Material	Density (g/cm ³)
Uniform configuration	SS304	7.80
	Inconel	8.40
	Hf	13.31
	AIC /	10.17
	Reduced radius AIC	
Non-uniform	AIC + SS304	
configuration	AIC + Inconel	-

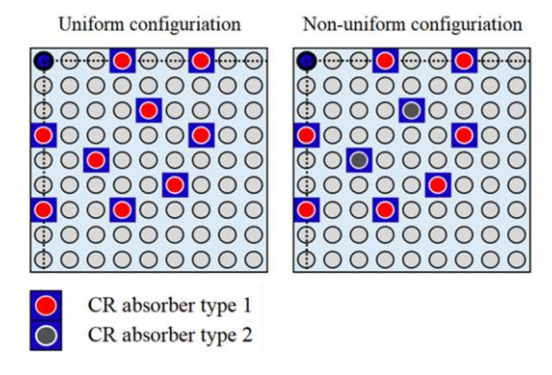


Fig. 2. Radial configurations of CR fingers (Uniform and Non-uniform) in a 1/4 FA

In this uniform configuration, SS304, Inconel, and reduced-radius AIC are introduced as gray rods, which have lower CR worth compared to conventional CRs and therefore mitigate axial power distribution distortion during CR movements. In the case of reduced-radius AIC, the clad outer diameter and thickness are maintained while the absorber radius varies from 0.25 to 0.35 cm in increments of 0.05 cm for sensitivity tests.

Hf was also included as a candidate. It has been employed in BWR CR assemblies and offers sufficient thermal neutron absorption capability in addition to its high melting point, irradiation stability, corrosion resistance, and mechanical properties [7], making it a promising candidate for long-term CR applications.

The non-uniform configuration, as illustrated on the right side of Fig. 2, refers to the case where different absorbing materials are combined within the CR fingers. Two combinations are considered: AIC + SS304 and AIC + Inconel. This concept can also be regarded as a gray rod arrangement, which has been adopted in LFO strategies such as Mode G and MSHIM [2]. In this

configuration, sensitivity tests are performed by progressively replacing the weak-absorber fingers, in sets of four, from positions 24 down to 4.

As illustrated in Fig. 3, the sensitivity test is performed by substituting each regulation bank (R4, R3, R2, R1) of the reference CR design with candidate materials. The subcriticality at CZP is then evaluated to observe the trend of the available margin (in pcm) with respect to the ARI criterion of 0.95, to assess the feasibility of applying these candidate materials.

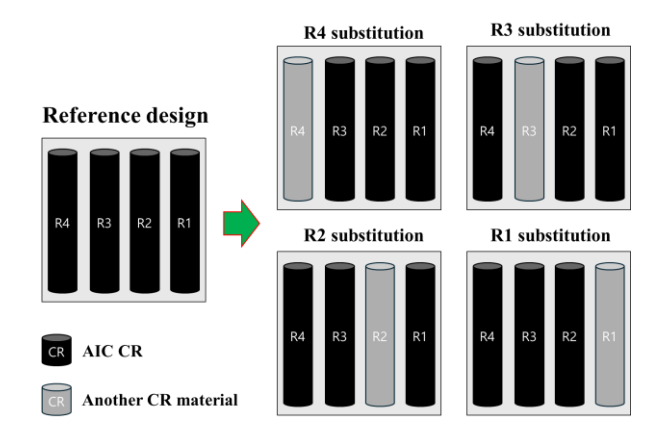


Fig. 3. Sensitivity test configurations: Substitution of Candidate Materials in each R Bank

3. Results and analysis

3.1 CZP subcriticality

Fig. 4 shows the margin to the ARI subcriticality limit under single-bank substitution with candidate materials (SS304, Inconel, and Hf), while the other banks remain as AIC. The green, red, blue, and black bars represent substitutions of the R4, R3, R2, and R1 banks, respectively. The red dashed line denotes the reference design described in Section 2.1, which maintains 1,618 pcm of margin to the ARI limit ($k_{\rm eff}$ =0.95). The value was calculated as (0.95 - current $k_{\rm eff}$) under CZP conditions at the beginning of cycle (BOC) of Cycle 1 and was reported in pcm unit.

When SS304 or Inconel is substituted for any R bank, the margin becomes negative, indicating that $k_{\rm eff}$ under CZP exceeds 0.95. In contrast, substitution with Hf consistently maintains a margin comparable to the reference design (1,618 pcm), satisfying the ARI requirement. These results demonstrate that Hf is a feasible alternative absorbing material, whereas SS304 and Inconel show limitations as replacements for the R banks.

Fig. 5 also shows the margin to the ARI subcriticality limit under single-bank substitution when varying the AIC radius (0.2~0.35 cm), while the other banks are maintained with the original AIC dimensions. Positive margins begin to appear at a radius of 0.25 cm. At 0.3 cm, the available margins are 625 pcm for R4 substitution, 753 pcm for R3, 385 pcm for R2, and 751 pcm for R1. When the radius is further increased to 0.35 cm, the

margins exceed approximately 1,000 pcm for all banks. Overall, the results indicate that the substitution of the R2 bank consistently yields the lowest margin compared to other banks, highlighting its greater sensitivity to such changes.

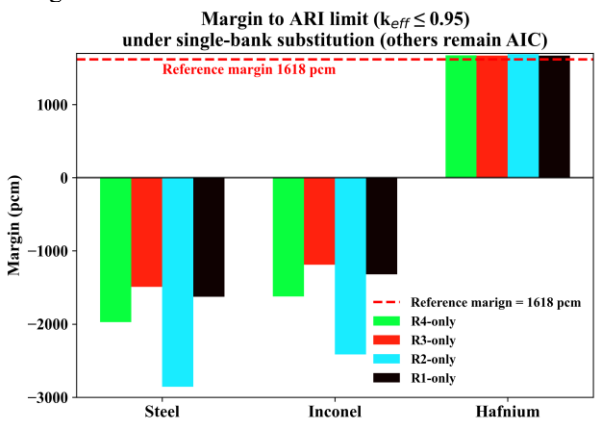


Fig. 4 Margin to ARI subcriticality limit under single-bank substitution with candidate CR Materials: (SS304, Inconel, Hf)

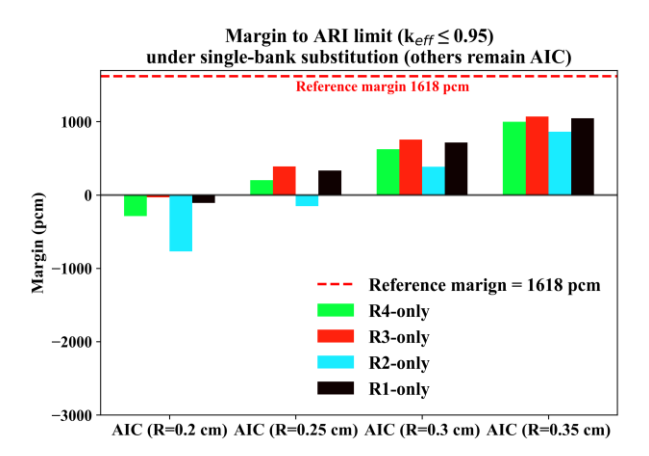


Fig. 5 Margin to ARI subcriticality limit under single-bank substitution with candidate CR Materials: (reduced-radius AIC, 0.20-0.35 cm)

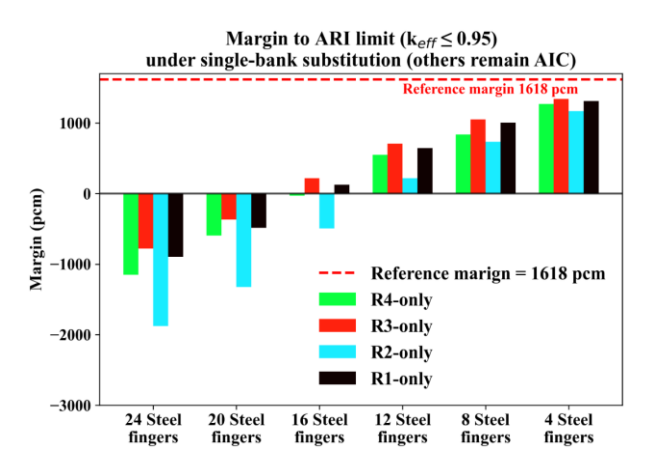


Fig. 6 Margin to ARI subcriticality limit under single-bank substitution with candidate CR Materials: (non-uniform SS304 fingers, $24 \rightarrow 4$)

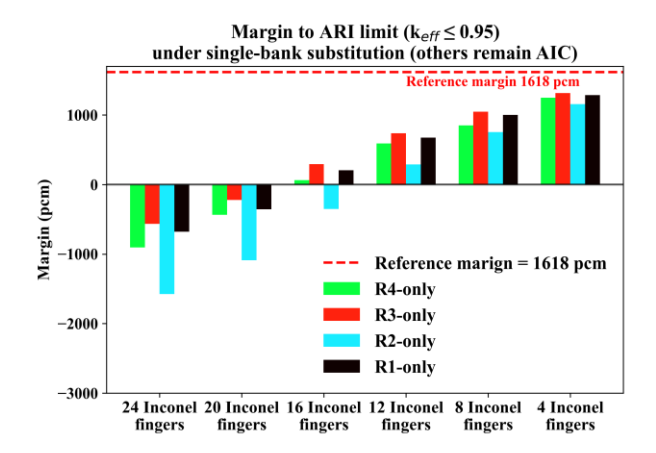


Fig. 7 Margin to ARI subcriticality limit under single-bank substitution with candidate CR Materials: (non-uniform Inconel fingers, $24 \rightarrow 4$)

Figs. 6 and 7 summarize the margins to the ARI subcriticality limit under single-bank substitution with non-uniform absorbing finger configuration. The overall trends are nearly identical. In both cases, the margin remains negative when the number of substituted fingers is large (20, 24 fingers). However, once the substitution is reduced to 16 fingers or fewer, a positive margin begins to appear. Especially, when only 8 fingers or fewer are replaced, the margin exceeds approximately 1,000 pcm, ensuring a modest subcriticality margin relative to the ARI limit.

3.2 Core Performances under HFP operation

In this section, the core performance is evaluated based on the feasibility results presented previously. Among the non-uniform configurations, the case of 20 AIC + 8 SS304 fingers was selected for preliminary analysis. Although this configuration achieves only ~70–80% of the CR reactivity worth of the baseline full black absorber (AIC) and thus does not strictly qualify as a gray rod, it maintains sufficient CR worth while leveraging the economic advantages of SS304, a lower-cost and more readily available material than AIC. Moreover, the reduced CR worth relative to the baseline is expected to moderate axial power tilts and improve axial power distribution control during operation.

In fact, as illustrated in Fig. 8, when the upper portion (\sim 120 cm) of the R1 bank-the last bank to be inserted-was replaced with enriched B₄C, the margin can be effectively recovered to 1,546 pcm, which is close to the reference design value of 1,618 pcm.

To evaluate the performance of this configuration, a preliminary case was considered in which the lead bank (R4) employed 20 AIC + 8 SS304 fingers, while the remaining banks (R3, R2, R1) were kept as AIC. This design was then compared against the reference case of All-AIC rods under the same insertion sequence and identical overlap lengths (OL)

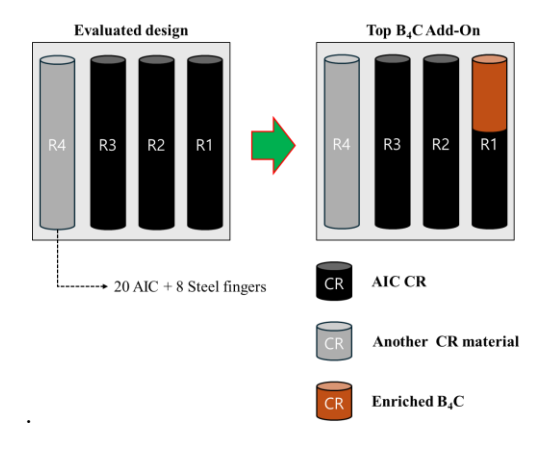
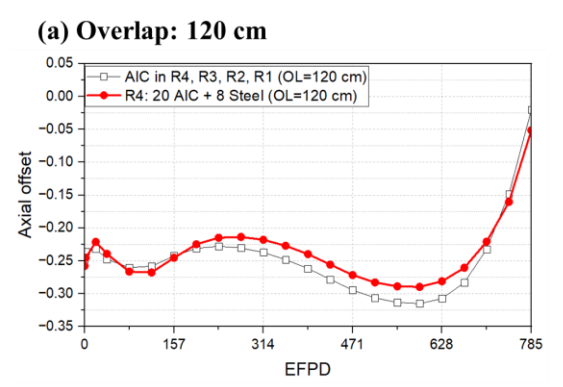
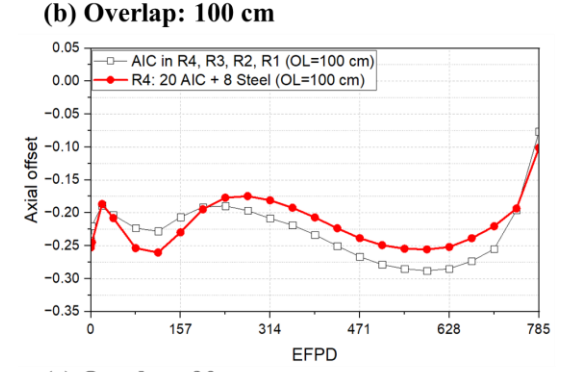


Fig. 8 Modified configuration for margin recovery

Comparison of axial offset at Equal CR Overlap: All-AIC vs. R4: 20 AIC + 8 Steel





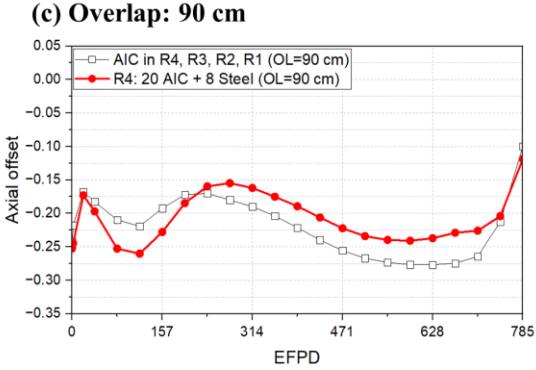
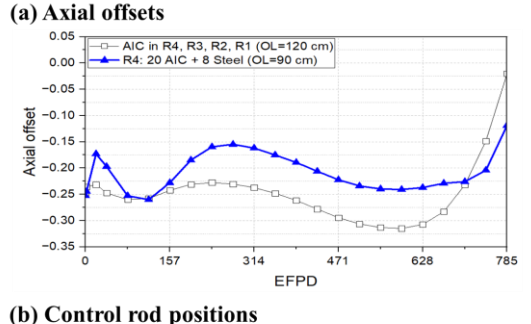
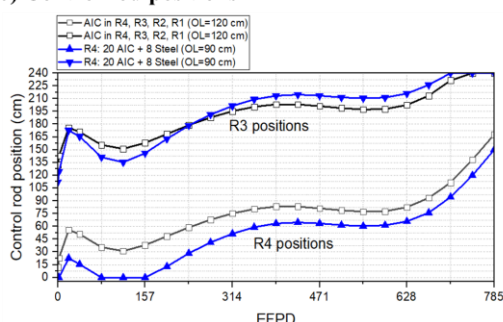


Fig. 9 Axial Offset comparison between reference (All AIC) and modified configuration (20 AIC + 8 SS304 in R4) for different overlap lengths.





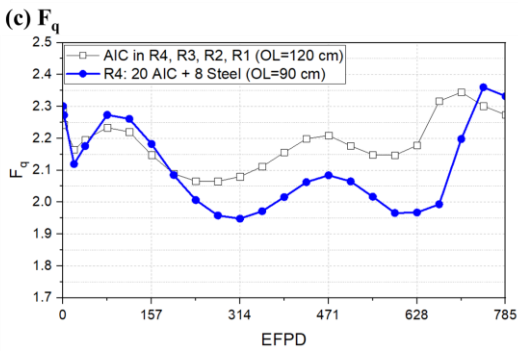


Fig. 10 Comparison of CR position, AO, and F_q evolutions between reference (All-AIC, OL = 120 cm) and non-unifrom configurations (WR4: 20 AIC + 8 SS304, OL = 90 cm)

Fig. 9 compares the axial offset (AO) evolution as a function of EFPD during the 1st cycle between the reference case (All-AIC rods in R4–R1) and the modified configuration (20 AIC + 8 SS304 in R4, AIC in R3–R1). Three OLs (OL = 120 cm, 100 cm, and 90 cm) are evaluated under identical control rod insertion sequences (R4 \rightarrow R3 \rightarrow R2 \rightarrow R1).

Across all three OL cases, the AO is observed to shift toward the upper core region in the EOC as the R4 and R3 banks are sequentially withdrawn. This trend becomes more pronounced with larger OL, since a deeper insertion of the follower bank (R3) reduces the distance between R4 and R3, thereby inducing a stronger upward shift in the axial power distribution during withdrawal. Conversely, smaller OL mitigates this axial power deviation, resulting in a more favorable axial power profile.

When comparing the two configurations under the same OL, the non-uniform case (R4: 20 AIC + 8 SS304) consistently exhibits smaller AO deviations than the reference (All-AIC). For instance, at OL = 120 cm, the AO swing (maximum-minimum) is reduced from 0.3021 in the reference to 0.2452 in the non-uniform case,

while at OL = 90 cm the values are further reduced to 0.1854 and 0.1477, respectively.

Fig. 10 summarizes an extreme comparison between the reference case (All-AIC, OL = 120 cm) and the non-uniform configuration (R4: 20 AIC + 8 SS304, OL = 90 cm). By adopting a non-uniform configuration and reducing the OL, the minimum-to-maximum AO deviation at the EOC can be reduced from 0.3021 to 0.1477, as shown in the figure. Although the R4 bank is inserted more deeply, the shorter OL with the R3 bank prevents the additional insertion of the R2 bank. For F_q , it stays lower until mid-cycle and shorter OL, and although it rises sharply near the EOC as the deeply inserted R4 bank is withdrawn, it remains within an acceptable design limit.

As an additional check, the performance of Hf rods—having a control worth like the reference design—was also examined. Fig. 11 shows that while the overall AO evolution is like AIC, the inherent material advantages of Hf, such as it's a similar neutron absorption cross section and excellent corrosion resistance, make it a promising alternative to AIC.

Overall, this study highlights that the choice of absorber material is a key optimization parameter in CR design for soluble boron-free i-SMR cores, providing a necessary foundation for subsequent investigations of other design parameters such as OL, grouping, and insertion strategies.

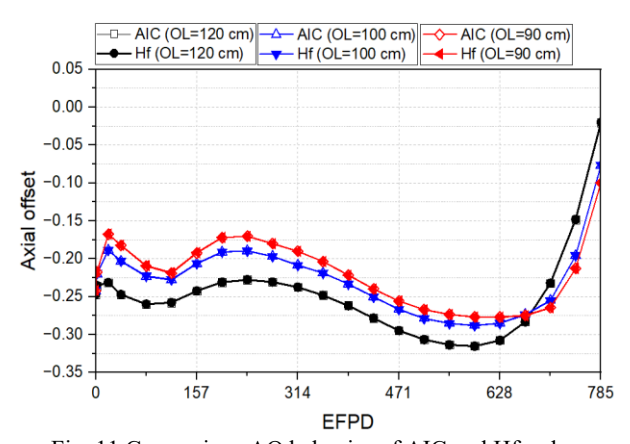


Fig. 11 Comparison AO behavior of AIC and Hf rods as a function of overlap length

4. Conclusions

In this work, neutronic evaluations of various CR materials were performed for application in a SBF i-SMR core. The results indicate that a non-uniform configuration such as 20 AIC + 8 SS304 rods can effectively reduce axial power deviations while maintaining sufficient shutdown margin.

In addition, Hf rods, which exhibit similar neutronic behavior to AIC, were shown to be a feasible alternative due to their favorable material properties.

These findings confirm that different absorber materials with comparable CR worth can serve as viable options for optimizing SBF i-SMR design.

Future work will focus on a more detailed

optimization of other CR parameters, including OL, insertion strategy, and grouping, to further enhance core performance and operational flexibility.

Acknowledgment

We are grateful to Jeong Woo Park at Kyung Hee University for his assistance in checking the input data. This paper was supported by the Innovative Small Modular Reactor Development Agency grant funded by the Korea Government (MOTIE) (No. RS-2024-00407975).

REFERECES

- [1] Kang, H. O., Lee, B. J., & Lim, S. G. (2024). Light water SMR development status in Korea. Nuclear Engineering and Design, 419, 112966.
- [2] OECD. Technical and economic aspects of load following with nuclear power plants. OECD Publishing, 2021.
- [3] J. Y. Cho, et al., "DeCART2D v1.1 User's Manual," KAERI/UM-40/2016, 2016.
- [4] J. Y. Cho, et al., "MASTER v4.0 User's Manual," KAERI/UM-41/2016, 2016.
- [5] Park, H. J., Kim, K. S., Hong, S. G., & Song, J. S. (2017). An improved DeCART library generation procedure with explicit resonance interference using continuous energy Monte Carlo calculation. *Annals of Nuclear Energy*, 105, 95-105.
- [6] Park, S., Seo, N., Kim, H., & Lee, J. Evaluation of the Flexible Operation Capability of an i-SMR Core Using RCS Outlet Temperature-Based Control Rod Operation Method.
- [7] Strasser, A. (2014). *Control assembly technology report: FMTR* (Vol. III). Advanced Nuclear Technology International (ANT International).